PNAS RESEARCH ARTICLE | PHYSIOLOGY

A RGS7-CaMKII complex drives myocyte-intrinsic and myocyte-extrinsic mechanisms of chemotherapy-induced cardiotoxicity

Madhuri Basak[a,1], Abhishek Singh Sengar[a,1], Kiran Das[a], Tarun Mahata[a], Manish Kumar[a], Dinesh Kumar[a], Sayan Biswas[b], Subhasish Sarkar[c], Pranesh Kumar[d], Priyadip Das[e], Adele Stewart[f], and Biswanath Maity[a,2]

Edited by Steven S. Rosenfeld, Mayo Clinic Minnesota, Jacksonville, FL; received August 19, 2022; accepted November 7, 2022 by Editorial Board Member Yale E. Goldman

Dose-limiting cardiotoxicity remains a major limitation in the clinical use of cancer chemotherapeutics. Here, we describe a role for Regulator of G protein Signaling 7 (RGS7) in chemotherapy-dependent heart damage, the demonstration for a functional role of RGS7 outside of the nervous system and retina. Though expressed at low levels basally, we observed robust up-regulation of RGS7 in the human and murine myocardium following chemotherapy exposure. In ventricular cardiomyocytes (VCM), RGS7 forms a complex with Ca^{2+}/calmodulin-dependent protein kinase (CaMKII) supported by key residues (K412 and P391) in the RGS domain of RGS7. In VCM treated with chemotherapeutic drugs, RGS7 facilitates CaMKII oxidation and phosphorylation and CaMKII-dependent oxidative stress, mitochondrial dysfunction, and apoptosis. Cardiac-specific RGS7 knockdown protected the heart against chemotherapy-dependent oxidative stress, fibrosis, and myocyte loss and improved left ventricular function in mice treated with doxorubicin. Conversely, RGS7 overexpression induced fibrosis, reactive oxygen species generation, and cell death in the murine myocardium that were mitigated following CaMKII inhibition. RGS7 also drives production and release of the cardiokine neuregulin-1, which facilitates paracrine communication between VCM and neighboring vascular endothelial cells (EC), a maladaptive mechanism contributing to VCM dysfunction in the failing heart. Importantly, while RGS7 was both necessary and sufficient to facilitate chemotherapy-dependent cytotoxicity in VCM, RGS7 is dispensable for the cancer-killing actions of these same drugs. These selective myocyte-intrinsic and myocyte-extrinsic actions of RGS7 in heart identify RGS7 as an attractive therapeutic target in the mitigation of chemotherapy-driven cardiotoxicity.

RGS protein | chemotherapy | cardiotoxicity | oxidative stress | cell death

Cancer therapy utilizes a multifaceted approach combining surgical resection, chemotherapy, and targeted therapies. Notably, chemotherapy improves patient survival over a 20-y period (1), but a series of potentially life-threatening side effects limits their clinical utility. Chemotherapy-induced cardiotoxicity is characterized by compromised left ventricular function, structural damage, conduction deficits, and vascular abnormalities and has been linked to anthracyclines (e.g., doxorubicin) and the antimetabolite 5-flurouracil (5-FU). Incidence rates for doxorubicin- and 5-FU-dependent heart damage vary based on drug schedule, age, cancer type, and cumulative dose and are estimated at 9% (2) and 1 to 19% (3), respectively. Monitoring of cardiac function in any patient receiving an anthracycline dose >200 mg/m^2 or for those at high risk of developing cardiac complications has a proven 93% sensitivity and 91% negative predictive value for future cardiotoxicity (4–6). Nevertheless, typical treatments for heart failure have been shown to normalize left ventricular ejection fraction (LVEF) in only 42% of patients (7), underscoring the need for more efficacious interventions.

Anthracycline-dependent inhibition of topoisomerase 2β activates the intrinsic mitochondrial cell death pathway (8) leading to oxidative stress and death of cardiomyocytes. Doxorubicin also drives reactive oxygen species (ROS) production via several DNA damage-independent mechanisms (9–12). Doxorubicin-dependent ROS also triggers Ca^{2+} leak due to induction of Ca^{2+}/calmodulin-dependent protein kinase (CaMKII) (13, 14). Cardiomyocytes are uniquely sensitive to oxidant damage as evident with high drug doses in glycolytic cells (15) because of their high metabolic demand and mitochondrial volume. Products of 5-FU metabolism also damage mitochondria in cardiomyocytes (16). However, 5-FU preferentially targets the vascular endothelium resulting in ischemia secondary to coronary spasm (17) and damages ECs by triggering ROS-dependent apoptosis (18). These data emphasize the potential contribution of extra-cardiac cell types to chemotherapy-induced cardiotoxicity. Indeed, doxorubicin-dependent oxidative stress drives transforming growth factor β1 (TGFβ1) release from cardiac fibroblasts, driving extracellular

Significance

Despite decades of clinical use, the utility of cancer chemotherapeutics is limited by adverse cardiac events. Although progress has been made in elucidating mechanisms underlying the pathogenesis of chemotherapy-dependent cardiotoxicity, the highly diverse rate of disease progression and lack of biomarkers have stymied efforts to prevent or reverse cardiac damage. Here, we identify RGS7, up-regulated in cardiac cells following chemotherapy exposure, as a key driver of chemotherapy-dependent oxidative stress, cell loss, and fibrosis in heart. Importantly, while RGS7 is both necessary and sufficient to drive chemotherapy-dependent heart damage, modulation of RGS7 expression in cancer cells fails to impact their sensitivity to chemotherapeutic drugs. Thus, RGS7 emerges as a potential therapeutic target in the detection or mitigation of chemotherapy-associated cardiac damage.

Author contributions: M.B., A.S.S., T.M., A.S., and B.M. designed research; M.B., A.S.S., K.D., T.M., M.K., D.K., S.B., S.S., P.K., and P.D. performed research; M.B., A.S.S., K.D., T.M., M.K., D.K., S.B., S.S., P.K., P.D., A.S., and B.M. analyzed data; and M.B., A.S.S., A.S., and B.M. wrote the paper.

The authors declare no competing interest.

This article is a PNAS Direct Submission. S.S.R. is a guest editor invited by the Editorial Board.

[1]M.B. and A.S.S. contributed equally to this work.

[2]To whom correspondence may be addressed. Email: bmaity@cbmr.res.in or bmaity28@gmail.com.

This article contains supporting information online at https://www.pnas.org/lookup/suppl/doi:10.1073/pnas.2213537120/-/DCSupplemental.

Published December 27, 2022.

matrix remodeling, collagen deposition, and the transformation of fibroblasts to profibrotic myofibroblasts (19). Paracrine factors such as neuregulin-1 (NRG1) are also released from the vascular endothelium influencing the survival and function of adjacent cardiomyocytes (20). Notably, targeting fibroblast or endothelial cell action protects against chemotherapy-induced cardiotoxicity in preclinical models (21, 22).

The R7 family of Regulator of G protein Signaling (RGS) proteins (RGS6, RGS7, RGS9, and RGS11) formco-stabilizing complexes with atypical G protein $G\beta_5$ (23). Knockdown of $G\beta_5$ in cardiomyocytes ameliorates chemotherapy-induced ROS generation, mitochondrial dysfunction, activation of ATM and CaMKII, and release of profibrotic factors from both ventricular cardiomyocytes (VCM) and ventricular cardiac fibroblasts (VCF) (24). However, $G\beta_5$ knockdown would be expected to destabilize all R7 family members present, and both RGS6 and RGS7 have been detected in heart (25). While RGS6 knockout protects against myocyte loss and activation of the DNA damage signaling in doxorubicin-treated VCM (26), the function of RGS7 in the myocardium remains unknown. Here, we identify RGS7, up-regulated following chemotherapy exposure, as a critical mediator of chemotherapy-induced cardiotoxicity. Among the RGS proteins expressed in heart, RGS7 has a unique function, forming a direct complex with CaMKII to mediate myocyte-intrinsic and myocyte-extrinsic pathology.

Results

RGS7 is Up-Regulated Following Chemotherapy Exposure. We acquired cardiac tissue samples during autopsy from patients with a history of chemotherapy and controls with no history of

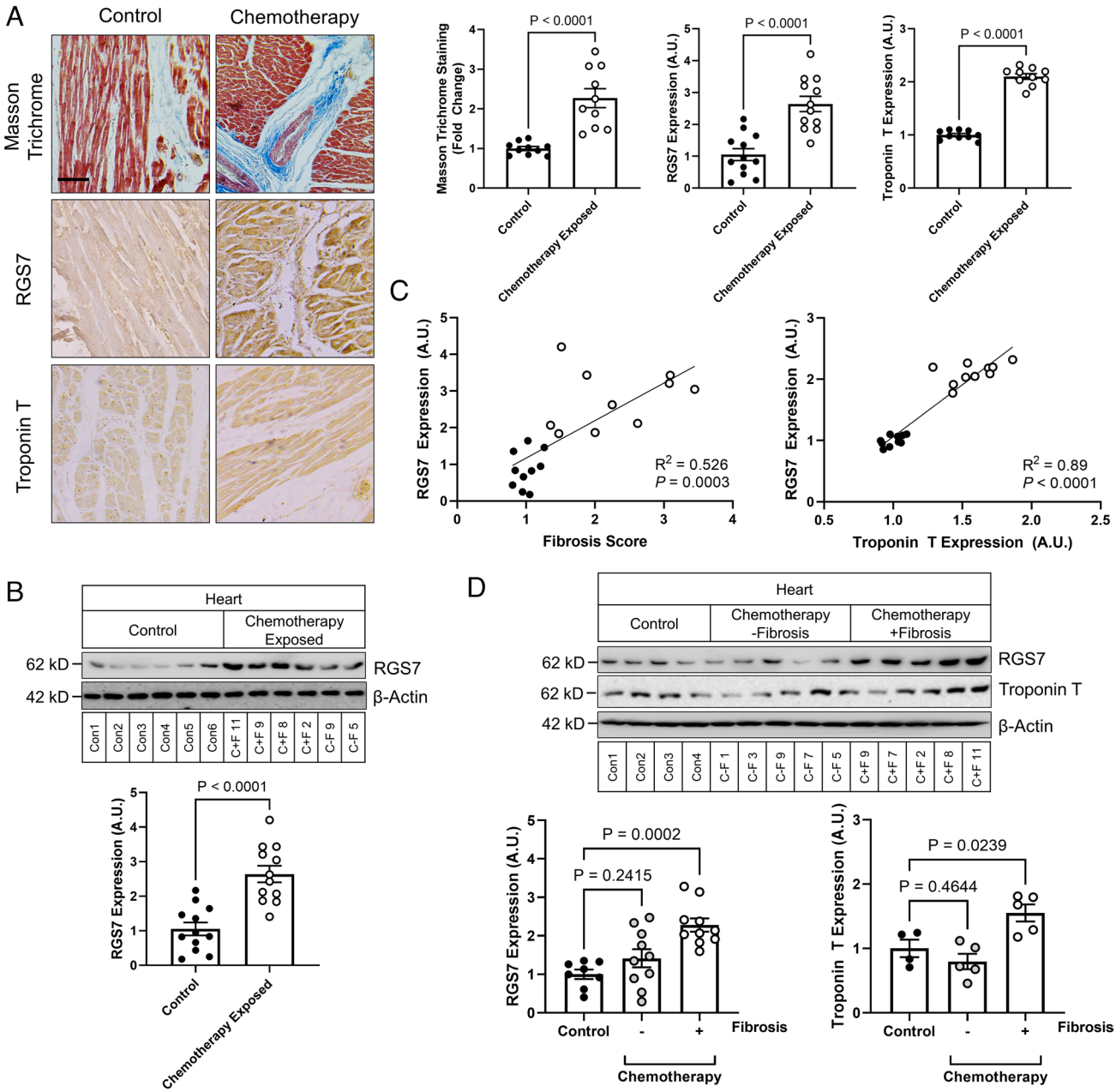

Fig. 1. RGS7 is up-regulated in the chemotherapy-exposed myocardium. (*A*) Cardiac staining (Scale bar, 100 μm.) and (*B*) correlation analysis for RGS7, Troponin T, and Masson trichrome in control or chemotherapy-exposed patients (n = 10). (*C*) RGS7 expression in heart tissue from chemotherapy-exposed patients or controls (n = 12). (*D*) RGS7 (n = 8 to 10) and Troponin T (n = 4 to 5) immunoreactivity in control and chemotherapy patients with/without detectable fibrosis. Codes corresponding to specific chemotherapy patients and controls (*SI Appendix*, Table S2) are provided. β-Actin serves as a loading control for immunoblots. Exact *P* values are provided on graphs. Data are presented as mean ± SEM.

cancer, chemotherapy, or cardiac issues (*SI Appendix*, Tables S1 and S2). Sections of myocardium from chemotherapy-treated patients displayed evidence of fibrotic remodeling (Fig. 1*A*) and aberrations in indicators of cardiac health (Fig. 1*A* and *SI Appendix*, Fig. S2*A*). Robust RGS7 protein up-regulation, as detected by both immunohistochemistry (Fig. 1*A*) and immunoblot (Fig. 1*B*), was also evident in hearts of chemotherapy patients, and, though to a lesser extent, following myocardial infarction (*SI Appendix*, Fig. S2*B*). There was also a significant correlation between RGS7 level and heart dysfunction (Fig. 1*C*). Not all patients undergoing chemotherapy display cardiotoxicity, and indeed, when we stratified our samples based on chemotherapy-treated individuals with or without detectable fibrosis, we noted a unique molecular signature in those displaying fibrotic remodeling characterized by RGS7 up-regulation (Fig. 1*D* and *SI Appendix*, Fig. S2*C*). We should note here that, while ejection fraction and chemotherapy duration did not differ significantly between the –fibrosis and +fibrosis groups, those patients displaying fibrotic remodeling were further removed from their chemotherapy treatment (*SI Appendix*, Table S1). Given the limitations of human heart specimens collected at autopsy and the correlational nature of these analyses, we cannot conclude based on these data whether the RGS7 up-regulation is specific to chemotherapy-dependent cardiac dysfunction or a universal marker of the failing myocardium precipitating our transition to model systems.

RGS7 Is Required for Doxorubicin-Dependent Mitochondrial Dysfunction and Cell Death in Murine VCM. Exposure of murine total heart cultures to the chemotherapeutic drugs doxorubicin or 5-FU resulted in RGS7 up-regulation (Fig. 2*A*). Based on prior work investigating the role of $G\beta_5$ in chemotherapy-dependent cardiotoxicity (24), we hypothesized that RGS7 might play a role in chemotherapy-driven mitochondrial dysfunction and cell death. Indeed, knockdown of RGS7 (Fig. 2*B*) was sufficient to prevent induction of antioxidants glutathione peroxidase (GPX) and superoxide dismutase (SOD) (Fig. 2*C* and *SI Appendix*, Fig. S3*B*), restore mitochondrial membrane potential ($\Delta\psi_M$) (Fig. 2*E* and *SI Appendix*, Fig. S3*D*), decrease accumulation of mitochondrial calcium (Fig. 2*D* and *SI Appendix*, Fig. S3*C*), and prevent cell loss (Fig. 2*F* and *SI Appendix*, Fig. S3*E*) in doxorubicin-treated VCM. Notably, RGS7 depletion proved equally efficacious at restoring mitochondrial bioenergetics at per with well-known mitochondrial calcium uniporter inhibitor Ru360 and mitochondrial permeability transition pore blocker cyclosporin A (Fig. 2 *D* and *E*). These two agents previously reported to impact mitochondrial bioenergetics significantly in different model systems.

RGS7 Interacts with CaMKII in Cardiomyocytes. $G\beta_5$ controls CaMKII-dependent apoptotic signaling (26), and thus, we hypothesized that RGS7 might also regulate CaMKII. Indeed, RGS7 and CaMKII form a co-immunoprecipitable complex in cardiomyocytes (Fig. 3*A*). Deletion of the catalytic RGS or Gγ-like (GGL) domain necessary for interaction with $G\beta_5$ impeded RGS7/CaMKII complex formation (Fig. 3*B*). In silico modeling of the RGS7/CaMKII complex identified three residues in RGS domain (P391, K412, and N398) predicted to support a high affinity direct interaction between RGS7/CaMKII (Fig. 3*C* and *SI Appendix*, Fig. S4). Mutation of two resides (P391 and K412) partially abolished RGS7-CaMKII co-precipitation (Fig. 3*D*).

We noted up-regulation and oxidation/phosphorylation of CaMKII in human chemotherapy patients (*SI Appendix*, Fig. S5 *A* and *B*). In the human myocyte cell line AC-16 (*SI Appendix*, Fig. S6*C*) or human-induced pluripotent stem cell (iPSC)-derived cardiomyocytes (chemotherapy treatment increased RGS7 expression and CaMKII phosphorylation. iPSC cardiomyocyte (Fig. 3 *E* and *F*) or AC-16 cells (*SI Appendix*, Fig. S5 *E* and *F*) apoptosis could be ameliorated through either RGS7 knockdown or CaMKII inhibition with KN-93, though the net impact of RGS7 depletion was greater (Fig. 3*E*). However, inhibition of CaMKII failed to improve cell survival in RGS7 KD cells indicating that RGS7 and CaMKII likely function in concert to drive myocyte cell death. We could phenocopy the impact of KN-93 in this system via specific knockdown of CaMKIIδ, the predominant cardiac CaMKII isoform (Fig. 3*F*). In addition, RGS7 overexpression (OE) was sufficient to increase ROS and induce cell death in iPSC-derived cardiomyocytes (*SI Appendix*, Fig. S5*G*), an effect that could be mitigated via inhibition of CaMKII. OE of wild type (WT) CaMKII or RGS7 in AC-16 cells triggered oxidative stress

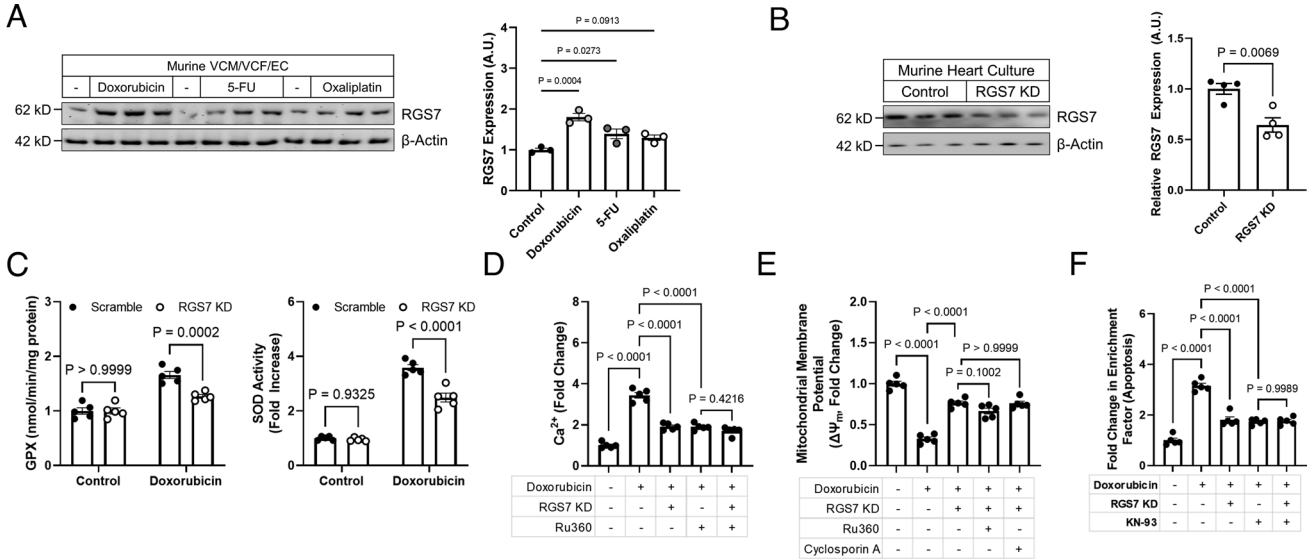

Fig. 2. RGS7 mediates doxorubicin-induced mitochondrial dysfunction, oxidative stress, and cell death. (*A*) RGS7 immunoreactivity in total heart cultures treated with doxorubicin (n = 3; 3 μM, 16 h), 5-FU (n = 3; 500 mM, 16 h), or oxaliplatin (n = 3; 0.06 mM, 16 h). (*B*) Verification of RGS7 knockdown in total heart cultures with scramble or RGS7-shRNA (n = 4). (*C*–*F*) Control or RGS7 knockdown (KD) VCM were treated with doxorubicin ± pre-treatment of Ru360 (50 μM, 1 h) or cyclosporin A (0.2 mM, 45 min). (*C*) GPX activity (n = 5) and SOD activity (n = 5). (*D*) Mitochondrial Ca^{2+} flux (n = 5). (*E*) $\Delta\psi_M$ (n = 5). (*F*) Apoptosis (cytoplasmic histone-associated DNA fragments; n = 5).

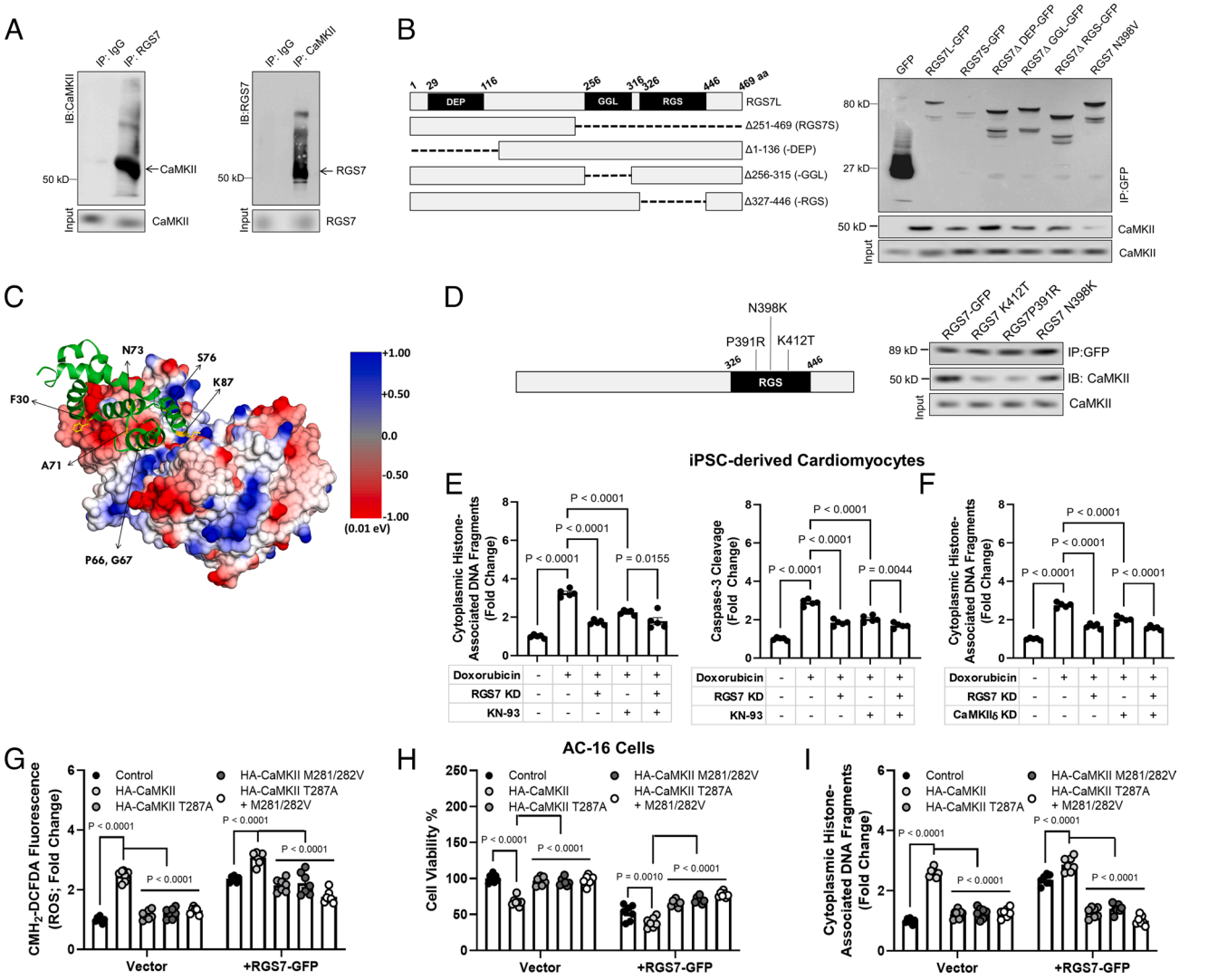

Fig. 3. RGS7 forms a complex with CaMKII and drives CaMKII-dependent cellular dysfunction. (*A*) Reciprocal co-IP of RGS7 and CaMKII in human AC-16 cardiomyocytes. (*B*) Co-IP of CaMKII with RGS7 deletion constructs. (*C*) In silico modeling of the RGS7-CaMKII complex revealed key RGS7 residues (K412, P391, N398) in the RGS domain of RGS7 predicted to support a direct RGS7/CaMKII interaction. (*D*) Mutation of specific residues abolishes RGS7-CaMKII binding. (*E* and *F*) Apoptosis was measure in control, or RGS7 KD human iPSC-derived cardiomyocytes (n = 5) were treated with doxorubicin (3 μM, 16 h) ± pre-treatment with CaMKII inhibitor KN-93 (*E*, 50 μM, 1 h) or δ-CaMKII shRNA (*F*). (*G–I*) AC-16 cells transfected with RGS7-GFP or control plasmid ± phosphorylation (T287A) or oxidation (M281/282V)-deficient CaMKII where indicated. (*G*) CM-H_2-DCFDA fluorescence (ROS; n = 7). (*H*) Cell viability (n = 7). (*I*) Apoptosis (n = 7).

(Fig. 4*G*), compromised cell viability (Fig. 4*H*), and induced apoptosis (Fig. 4*I*). We noted augmented RGS7-dependent ROS generation and cell death in cells expressing WT CaMKII (Figs. 3*I* and 4*G*), but not the phosphorylation (T287A) or oxidation (M281/282V)-deficient mutants, which almost completely attenuated RGS7-dependent myocyte cytotoxicity (Figs. 3*I* and 4*G*).

RGS7 Knockdown Protects against Chemotherapy-Induced Cardiotoxicity In Vivo. Chronic low-dose exposure to doxorubicin or 5-FU led to RGS7 induction in the murine heart that was accompanied by increased CaMKII phosphorylation and, to a lesser extent, oxidation (Fig. 4 *A* and *B*). Utilizing intracardiac administration, we achieved ~50% RGS7 knockdown in the murine myocardium (Fig. 4 *C* and *D* and *SI Appendix*, Fig. S6*B*), with no changes observed in liver or brain (*SI Appendix*, Fig. S6*A*). In mice treated chronically with doxorubicin, RGS7 depletion ameliorated fibrosis (Fig. 4 *E* and *F*), myocyte hypertrophy (Fig. 4 *E* and *G* and *SI Appendix*, Fig. S6*C*), and cardiac hypertrophy (Fig. 4*H* and *SI Appendix*, Fig. S6*D*). RGS7 knockdown also decreased doxorubicin-dependent ROS generation (Fig. 4*I*) and apoptosis (Fig. 4*J*) in heart. The impact of RGS7 depletion on markers of cardiac health translated to significant improvements in cardiac function tests (Fig. 4*K*).

Cardiac RGS7 OE Is Sufficient to Drive Myocyte Oxidative Stress and Apoptosis via a CaMKII-Dependent Mechanism. Cardiac RGS7 OE resulted in increased CaMKII phosphorylation, levels of cardiokines NRG1 and TGFβ1, and expression of alpha smooth muscle actin (αSMA), Atrial natriuretic peptide (ANP), and Myosin Heavy Chain Beta (β-MHC) (Fig. 5*A*). RGS7 was also sufficient to drive fibrosis (Fig. 5*B*), ROS generation (Fig. 5*C*), lost cell viability (Fig. 5*D*), and apoptosis (Fig. 5*E*) in heart. Administration of the CaMKII inhibitor KN-93 ameliorated RGS7-dependent molecular and histological aberrations (Fig. 5 *A–E*) indicating that the functional interaction between RGS7 and CaMKII is essential for ability of RGS7 to drive cardiotoxicity.

RGS7 Knockdown Impairs VCM/EC Crosstalk. Injury to the endothelium results in release of profibrotic/hypertrophic factors that propagate damage to the myocardium. Exposure of VCM

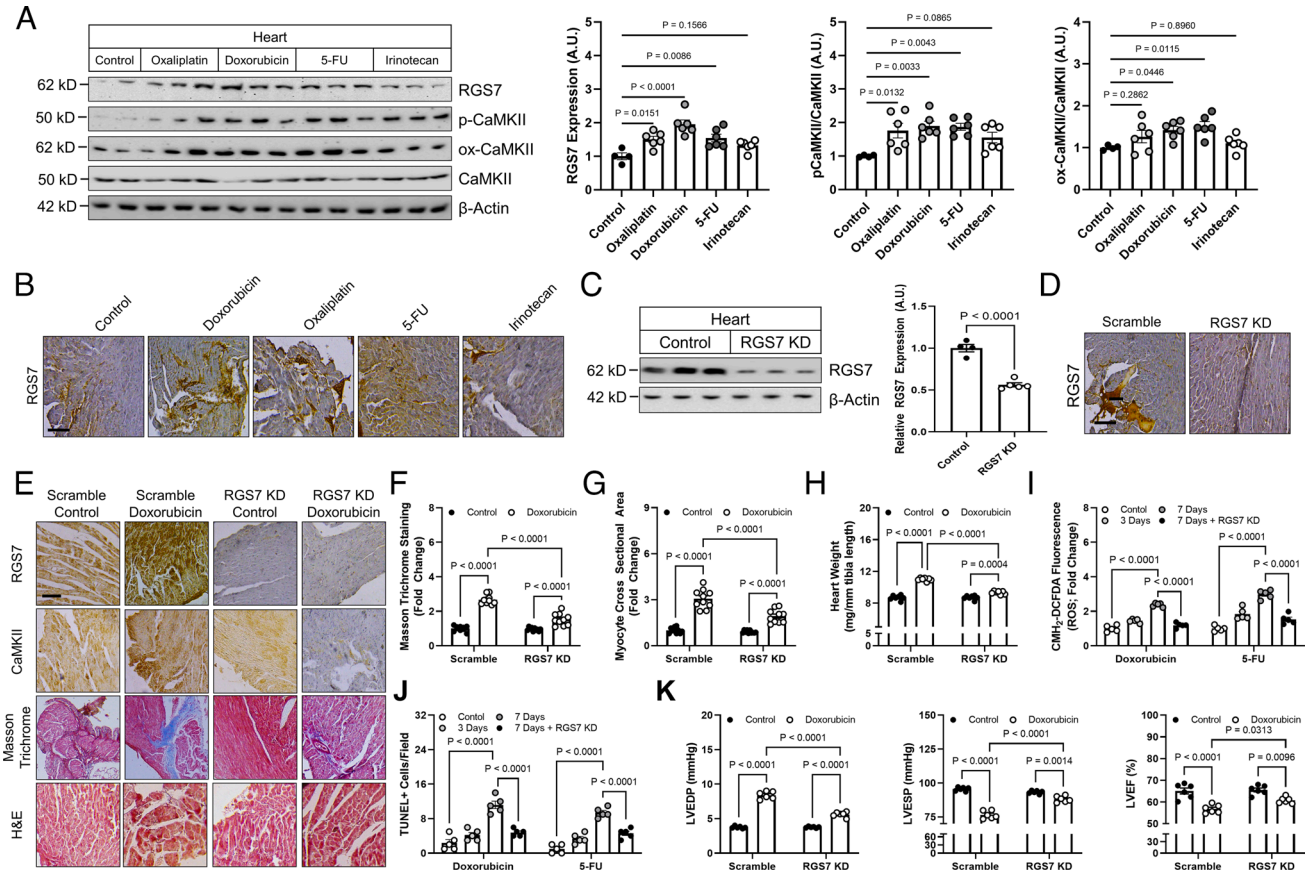

Fig. 4. Cardiac-specific RGS7 knockdown ameliorates chemotherapy-dependent cardiotoxicity in mice. (*A–H*, *K*) Following administration of scramble or RGS7-shRNA via intracardiac injection, mice were treated with doxorubicin (cumulative dose of 45 mg/kg i.p.), 5-FU (200 mg/kg i.p.), oxaliplatin (45 mg/kg i.p.), irinotecan (175 mg/kg i.p.), or saline control. After 8 wk, cardiac phenotyping was performed, and tissues collected 1 wk later for biochemical and histological analyses. (*A*) Immunoblotting for RGS7, p-CaMKII, and ox-CaMKII in heart (n = 6). (*B*) RGS7 immunohistochemistry in heart. (Scale bar, 100 μm.) RGS7 knockdown was verified in heart via (*C*) immunoblotting and (*D*) immunohistochemistry. (Scale bar, 100 μm.) (*E*) Representative images depicting RGS7, CaMKII, Masson trichrome (fibrosis), and H&E staining (myofibrillar architecture) in mice. (Scale bar, 100 μm.) Quantification of (*F*) fibrotic area (blue stain) from Masson trichrome (n = 10) and (*G*) myocyte area from H&E images (n = 10). (*H*) Heart weight (n = 10). (*I* and *J*) Mice were treated with single acute dose of doxorubicin (20mg/kg, i.p.), 5-FU (150 mg/kg, i.p.), oxaliplatin (30 mg/kg, i.p.), or saline control. (*I*) CM-H_2-DCFDA fluorescence (ROS; n = 5). (*J*) Quantification of TUNEL+ nuclei (apoptosis; n = 5). (*K*) Cardiac phenotyping (n = 6); left ventricular end diastolic and systolic pressure and LVEF.

to conditioned media from doxorubicin-treated endothelial cells (EC) or EC to conditioned media from doxorubicin-treated VCM resulted in RGS7 up-regulation (Fig. 6*B*). RGS7 knockdown in murine VCM was also sufficient to prevent CaMKII phosphorylation and oxidation, induction of the pathogenic inducible NOS (iNOS), NRG1 production, and phosphorylation of AKT following exposure of VCM monocultures to conditioned media from doxorubicin-treated EC (Fig. 6*C*). We obtained similar results following exposure of RGS7 KO AC-16 cells to media from doxorubicin-treated human HUVEC cells in each of two RGS7 KO clones (Fig. 6*D* and *SI Appendix*, Fig. S7*B*). Interestingly, exposure to conditioned media from doxorubicin-treated AC-16 cells increased only ox-CaMKII and not p-CaMKII in HUVEC cells (*SI Appendix*, Fig. S7*A*). In contrast, both p-CaMKII and ox-CaMKII increased in AC-16 cells (*SI Appendix*, Fig. S7*A*). Regardless of the direction of communication, RGS7 depletion in the originating cell type was sufficient to prevent both RGS7 induction and CaMKII activation in the recipient cell (*SI Appendix*, Fig. S7*A*). Given doxorubicin triggered rapid up-regulation of NRG1 in ECs, which represents the primary source of NRG1 in vivo (27), and prior evidence linking NRG1 to myocyte apoptosis (22), we hypothesized that NRG1 might be a key driver of EC to VCM crosstalk. Indeed, we could prevent RGS7 induction and CaMKII oxidation in VCM following transplantation of conditioned media from doxorubicin-treated EC by inhibiting NRG1 signaling with the erbB4 inhibitor cl-1033 (Fig. 6*E*).

RGS6, Not RGS7, Drives Cell Death Signaling in Breast Cancer Cells Following Doxorubicin Treatment. Anthracyclines are commonly incorporated into breast cancer treatment. Though RGS6 drives doxorubicin-induced cardiotoxicity (26), RGS6 also plays a key role in doxorubicin-dependent cancer cell apoptosis (28) and functions as a tumor suppressor (29). Modulating RGS7 levels in AC-16 cells via KD (*SI Appendix*, Fig. S8*A*) or OE (*SI Appendix*, Fig. S8*B*) had no impact on RGS6 expression. Consistent with prior reports (29), exposure of mice to the carcinogen DMBA results in decreased RGS6/Gβ_5 expression in breast tissue, but RGS7 remained unaltered (Fig. 7 *A* and *B*). Similarly, while OE of RGS6 increases ROS generation and apoptosis in breast cancer cell lines (30), RGS7 OE had no impact on cell survival (*SI Appendix*, Fig. S9*A*), colony formation (Fig. 7*C*), or oxidative stress and cell death (Fig. 7*D*). RGS7 knockdown also fails to impact cytotoxicity (Fig. 7*E*). RGS6 knockdown cripples the recruitment of the ATM/p53 DNA damage signaling cascade in cancer cells (Fig. 7*F* and *SI Appendix*, Fig. S9*B*). However, doxorubicin-dependent phosphorylation of Ataxia Telangiectasia Mutated (ATM) and p53 remains intact in both MDA-MB-231 (Fig. 7*G*) and MCF7 (*SI Appendix*, Fig. S9*C*)

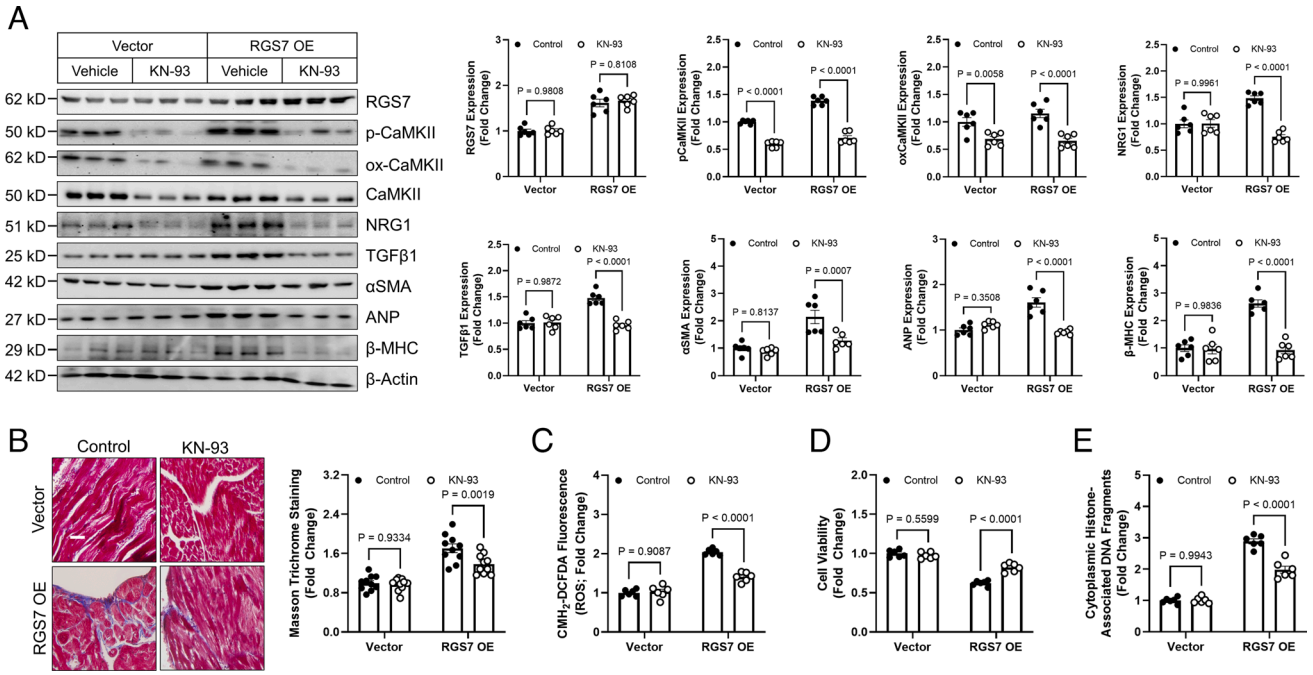

Fig. 5. RGS7 OE in heart is sufficient to drive CaMKII-dependent cardiotoxicity. A RGS7-containing viral construct or control was introduced into the myocardium. After 15 d, animals were given saline or KN-93 (8 mg/kg i.p. two doses, 4 d apart) and tissues collected 2 d after the last injection for downstream analyses. (*A*) Immunoblotting for RGS7, p-CaMKII, ox-CaMKII, NRG1, TGFβ1, αSMA, ANP, and β-MHC in cardiac tissue (n = 6). (*B*) Representative images and quantification of cardiac fibrosis (Masson trichrome staining; n = 6). (*C*) CM-H_2-DCFDA fluorescence (total ROS; n = 6). (*D*) Cell viability (n = 6). (*E*) Apoptosis (n = 6).

cells following RGS7 depletion. Thus, RGS6, not RGS7, is required for the cancer killing actions of doxorubicin.

Discussion

Though RGS7 mRNA was detected in heart over two decades ago, no studies have investigated the functional importance of RGS7 in the myocardium. We provide evidence that exposure to cancer chemotherapeutics, associated with dose-limiting and often irreversible cardiotoxicity, is associated with robust RGS7 up-regulation in the human heart. Indeed, cardiac-specific knockdown of RGS7 in mice protected the heart from doxorubicin-induced fibrosis, hypertrophy, oxidative stress, and apoptosis translating to significant improvements in cardiac function. In cardiomyocytes, RGS7 forms a complex with the pro-apoptotic kinase CaMKII and drives oxidative stress, mitochondrial dysfunction, and cell death. Whereas RGS7 OE in heart was sufficient to drive cell loss and fibrosis, inhibition of CaMKII provided partial protection. In addition to myocyte-intrinsic mechanisms of cytotoxicity, RGS7 also promotes select nodes of intercellular crosstalk, namely intercommunication between ECs and VCM, which could be decreased via RGS7 depletion in either the donor or recipient cell line in our in vitro model. Together these data identify the RGS7/CaMKII complex as a critical mediator of chemotherapy-induced cardiac damage.

CaMKII activity is controlled by two parallel signaling mechanisms. First, Ca^{2+} elevations trigger calmodulin binding to CaMKII holoenzyme resulting in exposure of a threonine residue on the autoinhibitory domain (T286), auto-phosphorylation, and activation (31). Second, CaMKII can also be directly activated via oxidation at a pair of methionine residues (M281/M282) in the regulatory domain (32). RGS7 facilitates both CaMKII oxidation and phosphorylation in VCM as evidenced by loss of chemotherapy-induced increases in p-CaMKII and ox-CaMKII in RGS7-deficient cells. However, when we overexpressed RGS7 in heart, we noted an increase in CaMKII phosphorylation, but not oxidation. Though RGS7/Gβ_5 complexes have been shown to suppress G-protein coupled receptor (GPCR)-dependent intracellular Ca^{2+} elevations, RGS7/Gβ_5 are also capable of facilitating Ca^{2+} influx via membrane-associated Ca^{2+} channels (33), providing a possible mechanism that may underlie RGS7-dependent CaMKII phosphorylation. Given that RGS7 and CaMKII form direct complex, RGS7 binding might also unmask autophosphorylation sites independent of both ROS and intracellular Ca^{2+}.

Our data have shown that RGS7 regulates intercommunication between VCM and vascular ECs. Chemotherapeutics induce oxidative stress in EC (34), and prior work has demonstrated that ROS accumulation leads to EC death, disruption of the endothelium barrier, and depletion of supportive paracrine factors released from EC to neighboring myocytes (20), which are in very close proximity in the capillary-rich myocardium (35). Depletion of RGS7 from either cell type provided marked protection against cell damage induced by transplantation of conditioned media from doxorubicin-treated donor cells. Thus, the protective impact of RGS7 blockade in the chemotherapy-exposed myocardium may derive from actions in both myocytes and ECs.

Though research into the role of NRG1 in chemotherapy-induced cardiotoxicity is in its infancy, prior work has suggested that, following acute exposure to high doses of doxorubicin, knockout of NRG1 or its receptor exacerbates cardiac injury (36, 37). Whereas acute doxorubicin appears to trigger NRG1 down-regulation (36, 37), our data demonstrate that chronic low-dose chemotherapy treatment or RGS7 OE increases NRG1 and TGFβ1 levels in heart, a phenotype consistent with what we observed in the hearts of human patients. Though seemingly paradoxical, these data are largely consistent with the known role of cytokines such as TGFβ1 in tissue remodeling following injury (38). In the acute stage immediately following cardiac damage, TGFβ1 plays a protective role initiating fibrotic remodeling and myofibroblast transdifferentiation

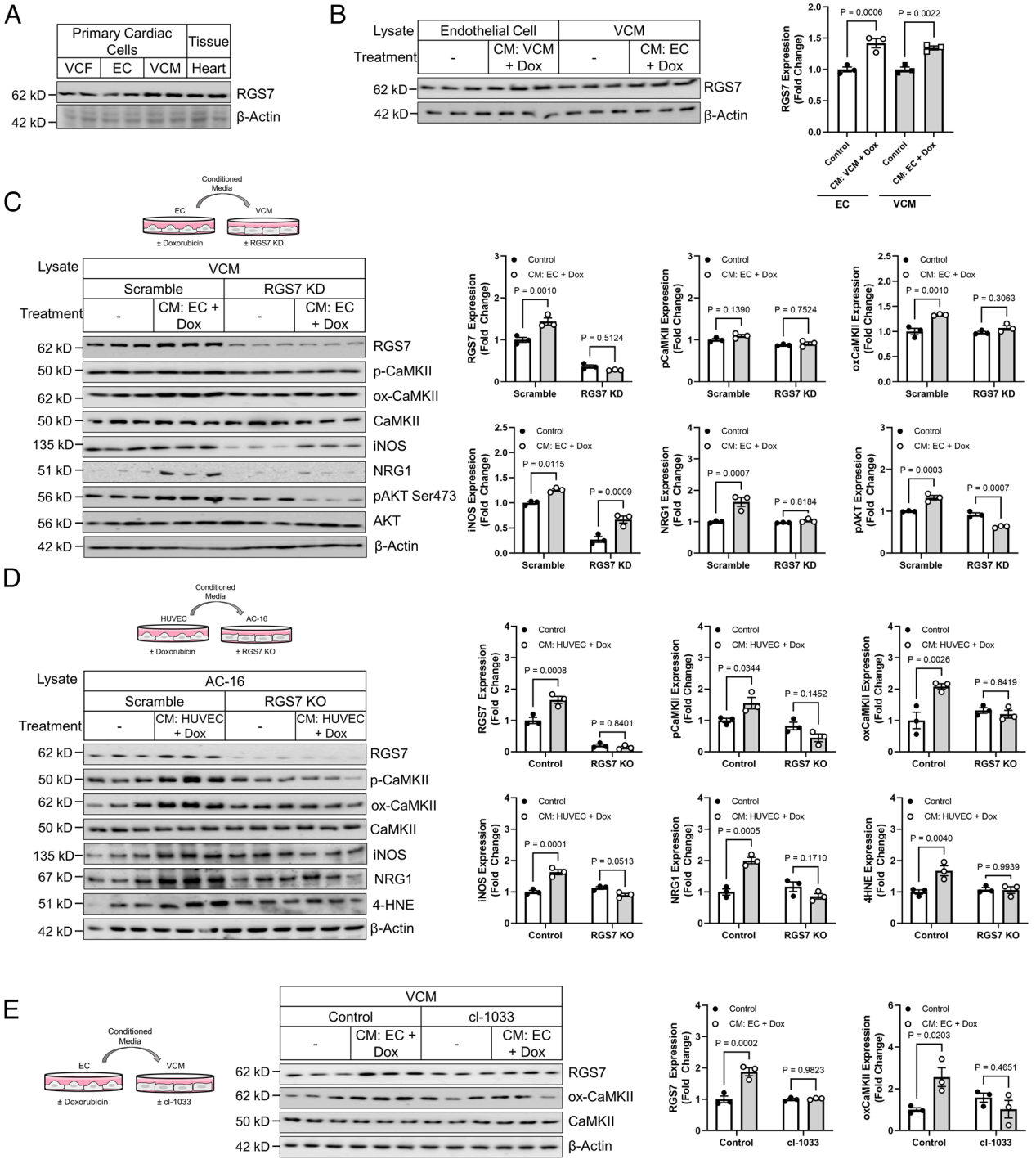

Fig. 6. RGS7 knockdown protects VCM from EC-driven myocyte dysfunction. (*A*) RGS7 expression in heart, VCM, VCF, and EC. (*B*) VCM and EC were treated with conditioned media from doxorubicin-treated (3 μM, 24 h) EC or VCM, respectively. Lysates were probed for RGS7 expression (n = 3). (*C*) Control or RGS7 KD VCM cultures (n = 3) were treated with conditioned media from doxorubicin-treated (3 μM, 24 h) EC and the resultant lysates were probed for RGS7, p-CaMKII, ox-CaMKII, iNOS, NRG1, and p-AKT. (*D*) Control or RGS7 KO AC-16 cardiomyocytes (n = 3) were treated with conditioned media from doxorubicin-treated (3 μM, 24 h) HUVEC cells, and immunoblotting was performed to detect RGS7, p-CaMKII, ox-CaMKII, iNOS, NRG1, and 4-HNE. (*E*) Murine ECs (n = 3) were treated with doxorubicin (3 μM, 24 h), and the culture media transplanted onto VCM cultures in the presence or absence of the tyrosine kinase inhibitor cl-1033 (2 μM, 1 h). RGS7, ox-CaMKII, and CaMKII expression were determined.

essential for maintenance of organ integrity. However, days following exposure, TGFβ1 levels rise, likely because of continued cardiac remodeling, and drive maladaptive fibrosis leading to compromised organ function (39–41). Indeed, in a clinical cohort, chemotherapy exposure was associated with an overall reduction in NRG1 levels, but higher than baseline NRG1 levels were observed in individuals with the most severe loss of cardiac function (42). A delayed response to chemotherapy exposure is also consistent with our observation that fibrotic remodeling was most pronounced in individuals several months removed from chemotherapy exposure even after controlling for total duration of treatment.

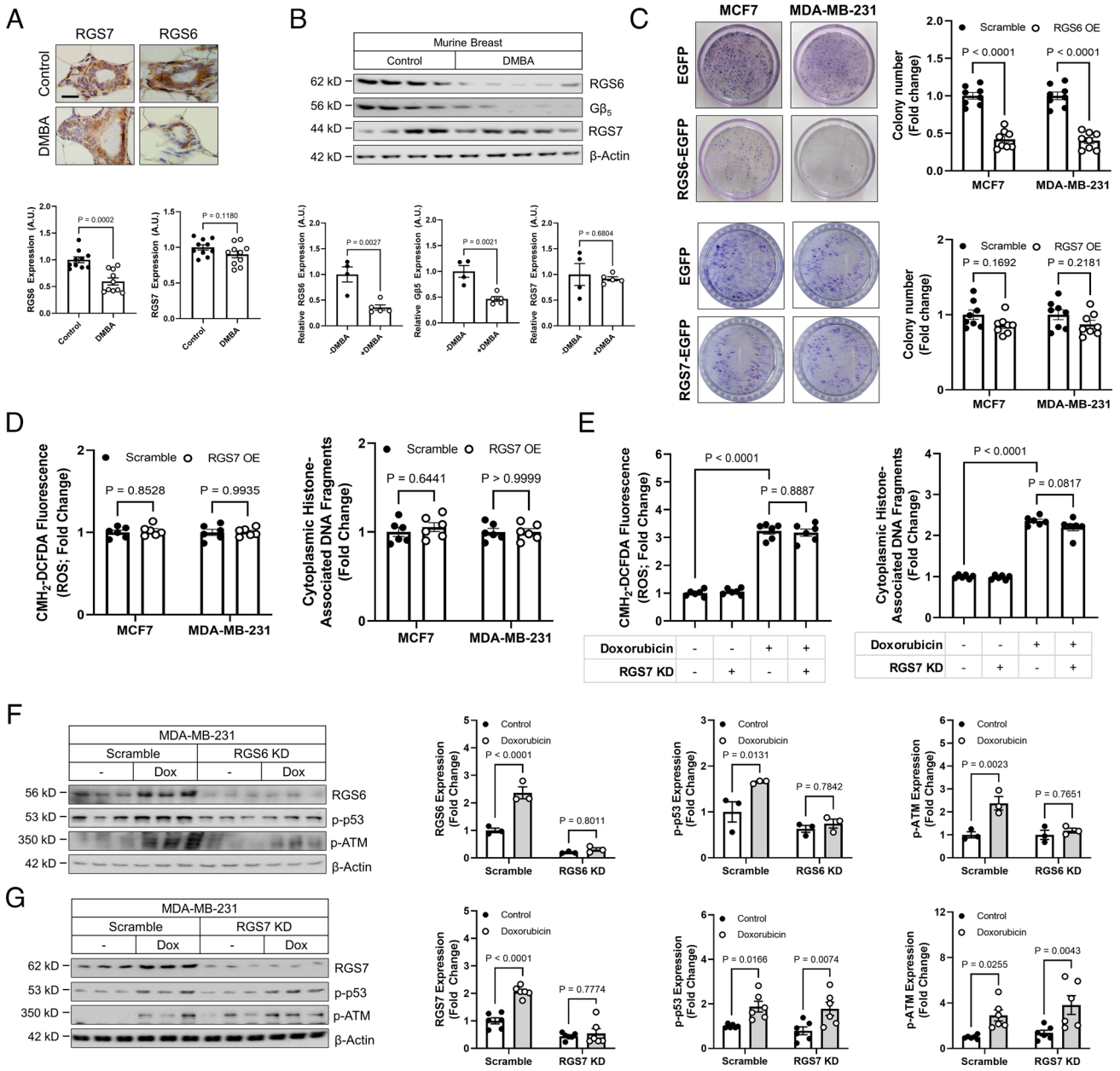

Fig. 7. RGS6, not RGS7, drives chemotherapy-dependent death of breast cancer cells. (*A* and *B*) Female mice (n = 10) were treated with the carcinogen DMBA (1 mg/20 g body weight), and protein expression detected in breast tissue via (*A*) immunohistochemistry (n = 10) and (*B*) immunoblot (n = 4 to 5). (*C*) Colony formation in MCF7 or MDA-MB-231 cells following transfection of control (GFP), RGS6-GFP or RGS7-GFP (n = 8). (*D*) RGS7-GFP was transfected into MCF7 or MDA-MB-231 breast cancer cells and CM-H_2-DCFDA fluorescence (total ROS; n = 6) and apoptosis (n = 6) measured. (*E*) MDA-MB-231 cells were treated with doxorubicin (2 μM, 12 h) following introduction of scramble or RGS7-shRNA and total ROS (n = 6); and apoptosis (n = 6) measured. MDA-MB-231 cells were treated with doxorubicin (2 μM, 12 h) following introduction of scramble or (*F*) RGS6- or (*G*) RGS7-shRNA. RGS6/7, p-p53, and p-ATM expression were determined.

R7 family members form a co-stabilizing complex with the atypical G protein $G\beta_5$, which had previously been implicated in doxorubicin-dependent cardiac damage (24). $RGS6^{-/-}$ mice are also protected against doxorubicin-dependent cardiotoxicity (26). $G\beta_5$, RGS6, and RGS7 are all up-regulated following administration of doxorubicin in mice (24, 26), though RGS7 is the only protein whose induction has now been observed in the human heart. Though the proteins share homology (~75%), RGS6 and RGS7 have unique, non-redundant functions. While both RGS6 and RGS7 drive oxidative stress and apoptosis, they do so via distinct mechanisms with RGS6, which forms a direct complex with ATM (43), modulating the ATM/p53 signaling cascade (26) and RGS7 facilitating activation of CaMKII (Fig. 8). Indeed, RGS6 (28, 30), but not RGS7, is pro-apoptotic and required for cytotoxic actions of doxorubicin in cancer cells. RGS6 possess potent anti-tumor actions particularly in breast cancer whose therapeutic regimens often utilize doxorubicin and/or 5-FU (29, 30, 44). Though RGS6 inhibition may protect the heart against chemotherapy-induced damage, it might also compromise the therapeutic efficacy of chemotherapy and/or drive de novo carcinogenesis. RGS6 also plays an important pace-making function in the heart where RGS6-dependent inhibition of G protein-coupled muscarinic M2 receptors functions as a break on parasympathetic drive (45, 46) and influences heart rate variability in mice (47) and humans (48). However, unlike RGS6, RGS7 expression does not change in breast following carcinogen exposure. While polymorphisms in the RGS7 gene have been identified in melanoma (49) and linked to patient survival in non-small cell lung cancer (50), RGS7 fails to impact the ability of doxorubicin to kill glycolytic breast cancer cells highlighting the advantage of RGS7 as a therapeutic target in chemotherapy-induced cardiotoxicity.

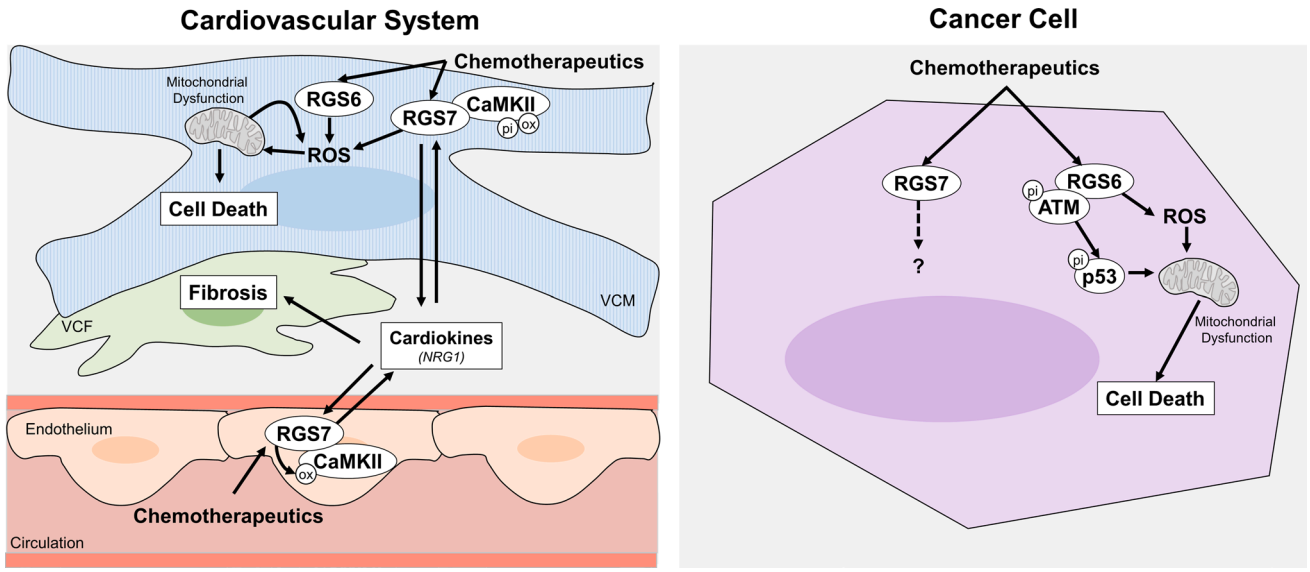

Fig. 8. Schematic diagram depicting the cardiac and extra-cardiac impacts of RGS7 following induction by chemotherapeutic drugs. Chemotherapeutic drugs lead to induction of RGS7/CaMKII in both ECs and ventricular cardiac myocytes. In VCM, RGS7 promotes oxidative stress, mitochondrial dysfunction, and cell death as well as the release of cardiokines that drive cardiac fibrosis and loss of ventricular integrity.

Materials and Methods

Materials. The source/catalog information for all reagents, antibodies, assay kits, and cell lines can be found in *SI Appendix*, Tables S3–S7.

Animals. Swiss albino mice (25 to 30 g) were reared on a balanced laboratory diet as per NIN, Hyderabad, India. They were kept at 20 ± 2 °C, 65 to 70% humidity, and day/night cycle (12 h/12 h). Unless otherwise noted, 8 to 10-wk-old male mice were utilized for experiments.

In Vivo RGS7 Knockdown (KD) or OE in Heart. 1-wk-old WT mice received a single intraventricular injection of 4.5×10^8 lentiviral vectors containing scramble or RGS7-targeted Short hairpin RNA (shRNA) (Santa Cruz Biotechnology) in a 40 μL volume according to a previously published protocol (51) or 70 μL of lentivirus containing 2×10^8 particles of either mRGS7-Lenti or a control empty vector virus. After injection, mice were returned to their mothers until weaning and allowed to age to adulthood (8 to 10 wk) for subsequent experiments. RGS7 knockdown and OE were verified via immunoblotting. Following intracardiac injection, body weight (1×/wk) and food intake (1 to 2×/wk) were monitored. No notable alterations in animal weight, food intake, or general well-being were found.

Protein Detection and Isolation. Immunoblotting, immunoprecipitation, and immunohistochemistry were performed according to previously published protocols (24). Additional details including dilutions for all antibodies used can be found in *SI Appendix*, Table S4.

Cell Isolation and Culture. Standard culture conditions for all commercially available cell lines can also be found in *SI Appendix*, Table S6. Primary VCM, EC, and VCF were isolated from 8 to 10-wk-old adult mice according to published protocols (52, 53). Cells were then transduced with lentiviral vectors according to the manufacturer's instructions with RGS7-targeted, CaMKIIδ-targeted, or scramble shRNA (Santacruz Biotechnology). RGS7, RGS7 deletion constructs, CaMKII, or CaMKII mutants were transfected where indicated.

Statistical Analyses. Data were analyzed by Student's *t* test (2 groups) or one- (1 variable, >2 groups) or two-way (2 variables, >2 groups) ANOVA with the Bonferroni post hoc adjustment. Statistical analyses were performed using Graphpad Prism software (v9). Results were considered significantly different at $P < 0.05$. Values are expressed as means ± SEM unless otherwise noted. Nominal *P*-values (*t*-test) or adjusted *P*-values (ANOVA) are provided on each graph.

Study Approval. Mouse experiments were performed at the Aryakul College of Pharmacy & Research, Lucknow, India. Animals were procured after obtaining clearance from the college Animal Ethics Committee (1896/PO/Re/S/16/CPCSEA/2021/5) and were handled following International Animal Ethics Committee Guidelines. Postmortem human tissue samples and serum samples were acquired from the Department of Forensic Medicine, Sagore Dutta Medical College & Hospital, Kolkata, West Bengal after obtaining the ethical clearance from the Centre of Biomedical Research Ethics Committee (Ref: IEC/CBMR/Corr/2020/16/6). Information on the sex, age, cause of death, comorbid conditions, and chemotherapy history for all heart autopsy samples is available in *SI Appendix*, Table S2.

Additional methodological details can be found in the *SI Appendix*, Data Supplement.

Data, Materials, and Software Availability. All study data are included in the article and/or *SI Appendix*.

ACKNOWLEDGMENTS. We acknowledge funds from CBMR, Department of Medical education, Uttar Pradesh Government (CBMR/IMR/0014/2022), Department of Biotechnology (DBT-BT/PR28635/MED/30/2145/2019), Indian Council of Medical Research (ICMR-5/4/1-26/2020-NCD-I), and DRDO (DG-(TM)/81/48222/LSRB-307/SH&DD&BD/2017) India to B.M.

Author affiliations: [a]Centre of Biomedical Research, Sanjay Gandhi Postgraduate Institute of Medical Sciences (SGPGIMS) Campus, Lucknow, Uttar Pradesh 226014, India; [b]Forensic Medicine, College of Medicine and Sagore Dutta Hospital, Kolkata, West Bengal 700058, India; [c]Surgery, College of Medicine and Sagore Dutta Hospital, Kolkata, West Bengal 700058, India; [d]Pharmaceutical Sciences, Aryakul College of Pharmacy & Research, Lucknow, Uttar Pradesh 226002, India; [e]Chemistry, SRM Institute of Science and Technology, Kattankulathur, Tamilnadu 603203, India; and [f]Biomedical Science, Charles E. Schmidt College of Medicine, Florida Atlantic University, Jupiter, FL 33458

1. D. K. Shakir, K. I. Rasul, Chemotherapy induced cardiomyopathy: Pathogenesis, monitoring and management. *J. Clin. Med. Res.* **1**, 8–12 (2009).
2. P. A. Henriksen, Anthracycline cardiotoxicity: An update on mechanisms, monitoring and prevention. *Heart* **104**, 971–977 (2018).
3. T. Shiga, M. Hiraide, Cardiotoxicities of 5-Fluorouracil and other fluoropyrimidines. *Curr. Treat. Options Oncol.* **21**, 27 (2020).
4. D. Cardinale *et al.*, Prognostic value of troponin I in cardiac risk stratification of cancer patients undergoing high-dose chemotherapy. *Circulation* **109**, 2749–2754 (2004).
5. D. J. Lenihan *et al.*, The utility of point-of-care biomarkers to detect cardiotoxicity during anthracycline chemotherapy: A feasibility study. *J. Card Fail* **22**, 433–438 (2016).
6. T. Negishi, P. Thavendiranathan, K. Negishi, T. H. Marwick, S. Investigators, Rationale and design of the strain surveillance of chemotherapy for improving cardiovascular outcomes: The SUCCOUR trial. *JACC Cardiovasc. Imaging* **11**, 1098–1105 (2018).
7. D. Cardinale, F. Iacopo, C. M. Cipolla, Cardiotoxicity of anthracyclines. *Front. Cardiovasc. Med.* **7**, 26 (2020).
8. A. C. Childs, S. L. Phaneuf, A. J. Dirks, T. Phillips, C. Leeuwenburgh, Doxorubicin treatment in vivo causes cytochrome C release and cardiomyocyte apoptosis, as well as increased mitochondrial

efficiency, superoxide dismutase activity, and Bcl-2: Bax ratio. *Cancer Res.* **62**, 4592–4598 (2002).
9. K. J. Davies, J. H. Doroshow, Redox cycling of anthracyclines by cardiac mitochondria. I. Anthracycline radical formation by NADH dehydrogenase. *J. Biol. Chem.* **261**, 3060–3067 (1986).
10. J. H. Doroshow, K. J. Davies, Redox cycling of anthracyclines by cardiac mitochondria. II. Formation of superoxide anion, hydrogen peroxide, and hydroxyl radical. *J. Biol. Chem.* **261**, 3068–3074 (1986).
11. G. Minotti *et al.*, Doxorubicin cardiotoxicity and the control of iron metabolism: Quinone-dependent and independent mechanisms. *Methods Enzymol.* **378**, 340–361 (2004).
12. Y. Zhao *et al.*, Nox2 NADPH oxidase promotes pathologic cardiac remodeling associated with Doxorubicin chemotherapy. *Cancer Res.* **70**, 9287–9297 (2010).
13. C. M. Sag, A. C. Kohler, M. E. Anderson, J. Backs, L. S. Maier, CaMKII-dependent SR Ca leak contributes to doxorubicin-induced impaired Ca handling in isolated cardiac myocytes. *J. Mol. Cell Cardiol.* **51**, 749–759 (2011).
14. H. Tscheschner *et al.*, CaMKII activation participates in doxorubicin cardiotoxicity and is attenuated by moderate GRP78 overexpression. *PLoS One* **14**, e0215992 (2019).
15. G. Minotti, P. Menna, E. Salvatorelli, G. Cairo, L. Gianni, Anthracyclines: Molecular advances and pharmacologic developments in antitumor activity and cardiotoxicity. *Pharmacol Rev.* **56**, 185–229 (2004).
16. M. R. Eskandari, F. Moghaddam, J. Shahraki, J. Pourahmad, A comparison of cardiomyocyte cytotoxic mechanisms for 5-fluorouracil and its pro-drug capecitabine. *Xenobiotica* **45**, 79–87 (2015).
17. R. Hayward *et al.*, Training enhances vascular relaxation after chemotherapy-induced vasoconstriction. *Med. Sci. Sports Exerc.* **36**, 428–434 (2004).
18. C. Focaccetti *et al.*, Effects of 5-fluorouracil on morphology, cell cycle, proliferation, apoptosis, autophagy and ROS production in endothelial cells and cardiomyocytes. *PLoS One* **10**, e0115686 (2015).
19. D. Cappetta *et al.*, SIRT1 activation attenuates diastolic dysfunction by reducing cardiac fibrosis in a model of anthracycline cardiomyopathy. *Int. J. Cardiol.* **205**, 99–110 (2016).
20. A. Z. Luu *et al.*, Role of endothelium in doxorubicin-induced cardiomyopathy. *JACC Basic Transl. Sci.* **3**, 861–870 (2018).
21. H. Zhan *et al.*, Ataxia telangiectasia mutated in cardiac fibroblasts regulates doxorubicin-induced cardiotoxicity. *Cardiovasc Res.* **110**, 85–95 (2016).
22. T. An *et al.*, Neuregulin-1 protects against doxorubicin-induced apoptosis in cardiomyocytes through an Akt-dependent pathway. *Physiol. Res.* **62**, 379–385 (2013).
23. C. K. Chen *et al.*, Instability of GGL domain-containing RGS proteins in mice lacking the G protein beta-subunit Gbeta5. *Proc. Natl. Acad. Sci. U.S.A.* **100**, 6604–6609 (2003).
24. S. Chakraborti *et al.*, Atypical G protein beta5 promotes cardiac oxidative stress, apoptosis, and fibrotic remodeling in response to multiple cancer chemotherapeutics. *Cancer Res.* **78**, 528–541 (2018).
25. T. Kardestuncer, H. Wu, A. L. Lim, E. J. Neer, Cardiac myocytes express mRNA for ten RGS proteins: Changes in RGS mRNA expression in ventricular myocytes and cultured atria. *FEBS Lett.* **438**, 285–288 (1998).
26. J. Yang *et al.*, G-protein inactivator RGS6 mediates myocardial cell apoptosis and cardiomyopathy caused by doxorubicin. *Cancer Res.* **73**, 1662–1667 (2013).
27. K. Lemmens, K. Doggen, G. W. De Keulenaer, Role of neuregulin-1/ErbB signaling in cardiovascular physiology and disease: Implications for therapy of heart failure. *Circulation* **116**, 954–960 (2007).
28. J. Huang, J. Yang, B. Maity, D. Mayuzumi, R. A. Fisher, Regulator of G protein signaling 6 mediates doxorubicin-induced ATM and p53 activation by a reactive oxygen species-dependent mechanism. *Cancer Res.* **71**, 6310–6319 (2011).
29. B. Maity *et al.*, Regulator of G protein signaling 6 is a novel suppressor of breast tumor initiation and progression. *Carcinogenesis* **34**, 1747–1755 (2013).
30. B. Maity *et al.*, Regulator of G protein signaling 6 (RGS6) induces apoptosis via a mitochondrial-dependent pathway not involving its GTPase-activating protein activity. *J. Biol. Chem.* **286**, 1409–1419 (2011).
31. R. C. Rich, H. Schulman, Substrate-directed function of calmodulin in autophosphorylation of Ca2+/calmodulin-dependent protein kinase II. *J. Biol. Chem.* **273**, 28424–28429 (1998).
32. J. R. Erickson *et al.*, A dynamic pathway for calcium-independent activation of CaMKII by methionine oxidation. *Cell* **133**, 462–474 (2008).
33. D. Karpinsky-Semper, C. H. Volmar, S. P. Brothers, V. Z. Slepak, Differential effects of the Gbeta5-RGS7 complex on muscarinic M3 receptor-induced Ca2+ influx and release. *Mol. Pharmacol.* **85**, 758–768 (2014).
34. S. Kotamraju, E. A. Konorev, J. Joseph, B. Kalyanaraman, Doxorubicin-induced apoptosis in endothelial cells and cardiomyocytes is ameliorated by nitrone spin traps and ebselen. Role of reactive oxygen and nitrogen species. *J. Biol. Chem.* **275**, 33585–33592 (2000).
35. W. C. Aird, Phenotypic heterogeneity of the endothelium: II. Representative vascular beds. *Circ. Res.* **100**, 174–190 (2007).
36. F. F. Liu *et al.*, Heterozygous knockout of neuregulin-1 gene in mice exacerbates doxorubicin-induced heart failure. *Am. J. Physiol. Heart Circ. Physiol.* **289**, H660–H666 (2005).
37. Y. Y. Zhao *et al.*, Neuregulins promote survival and growth of cardiac myocytes. Persistence of ErbB2 and ErbB4 expression in neonatal and adult ventricular myocytes. *J. Biol. Chem.* **273**, 10261–10269 (1998).
38. W. A. Border, N. A. Noble, Transforming growth factor beta in tissue fibrosis. *N. Engl. J. Med.* **331**, 1286–1292 (1994).
39. S. M. Tan, Y. Zhang, K. A. Connelly, R. E. Gilbert, D. J. Kelly, Targeted inhibition of activin receptor-like kinase 5 signaling attenuates cardiac dysfunction following myocardial infarction. *Am. J. Physiol. Heart Circ. Physiol.* **298**, H1415–H1425 (2010).
40. H. Okada *et al.*, Postinfarction gene therapy against transforming growth factor-beta signal modulates infarct tissue dynamics and attenuates left ventricular remodeling and heart failure. *Circulation* **111**, 2430–2437 (2005).
41. R. M. Liu, L. P. Desai, Reciprocal regulation of TGF-beta and reactive oxygen species: A perverse cycle for fibrosis. *Redox Biol.* **6**, 565–577 (2015).
42. C. A. Geisberg *et al.*, Circulating neuregulin during the transition from stage A to stage B/C heart failure in a breast cancer cohort. *J. Card Fail.* **19**, 10–15 (2013).
43. T. Mahata *et al.*, Hepatic regulator of G protein signaling 6 (RGS6) drives non-alcoholic fatty liver disease by promoting oxidative stress and ATM-dependent cell death. *Redox Biol.* **46**, 102105 (2021).
44. J. Huang *et al.*, RGS6 suppresses Ras-induced cellular transformation by facilitating Tip60-mediated Dnmt1 degradation and promoting apoptosis. *Oncogene* **33**, 3604–3611 (2014).
45. J. Yang *et al.*, RGS6, a modulator of parasympathetic activation in heart. *Circ. Res.* **107**, 1345–1349 (2010).
46. E. Posokhova, N. Wydeven, K. L. Allen, K. Wickman, K. A. Martemyanov, RGS6/Gbeta5 complex accelerates IKACh gating kinetics in atrial myocytes and modulates parasympathetic regulation of heart rate. *Circ Res.* **107**, 1350–1354 (2010).
47. E. Posokhova *et al.*, Essential role of the m2R-RGS6-IKACh pathway in controlling intrinsic heart rate variability. *PLoS One* **8**, e76973 (2013).
48. I. M. Nolte *et al.*, Genetic loci associated with heart rate variability and their effects on cardiac disease risk. *Nat. Commun.* **8**, 15805 (2017).
49. N. Qutob *et al.*, RGS7 is recurrently mutated in melanoma and promotes migration and invasion of human cancer cells. *Sci. Rep.* **8**, 653 (2018).
50. J. Dai *et al.*, Genetic variations in the regulator of G-protein signaling genes are associated with survival in late-stage non-small cell lung cancer. *PLoS One* **6**, e21120 (2011).
51. S. Der Sarkissian *et al.*, Cardiac overexpression of angiotensin converting enzyme 2 protects the heart from ischemia-induced pathophysiology. *Hypertension* **51**, 712–718 (2008).
52. C. S. Long, C. J. Henrich, P. C. Simpson, A growth factor for cardiac myocytes is produced by cardiac nonmyocytes. *Cell Regul.* **2**, 1081–1095 (1991).
53. K. Jelonek *et al.*, Cardiac endothelial cells isolated from mouse heart - a novel model for radiobiology. *Acta. Biochim. Pol.* **58**, 397–404 (2011).